

Topological interpretation of color exchange invariants

O. Cépas^{1*}, P. M. Akhmetiev^{2,3}

1 Université Grenoble Alpes, CNRS, Grenoble INP, Institut Néel, 38000 Grenoble, France

2 HSE Tikhonov Moscow Institute of Electronics and Mathematics, 34 Tallinskaya Str.,
123458, Moscow, Russia

3 Pushkov Institute of Terrestrial Magnetism, Ionosphere and Radio Wave Propagation,
Kaluzhskoe Hwy 4, 108840, Moscow, Troitsk, Russia

* olivier.cepas@neel.cnrs.fr

Abstract

We explain a correspondence between some invariants in the dynamics of color exchange in a 2d coloring problem, which are polynomials of winding numbers, and linking numbers in 3d. One invariant is visualized as linking of lines on a special surface with Arf-Kervaire invariant one, and is interpreted as resulting from an obstruction to transform the surface into its chiral image with special continuous deformations. We also consider additional constraints on the dynamics and see how the surface is modified.

Contents

1	Introduction	2
2	Invariants of 2d flux lines dynamics	3
2.1	Dynamics I	3
2.2	Dynamics II	5
2.2.1	Additional invariants of the even sector.	6
3	Definition of the linking number	9
3.1	Linking number on the standard torus in 3d	9
3.2	Linking number on the double cover of the torus	10
3.3	Linking number on an arbitrary immersion of the torus	11
3.4	A topological invariant	12
4	Two classes of immersed torus	12
5	Invariant as a linking number	14
5.1	Construction of a Arf-Kervaire one, “ ∞ -perfect”, immersed torus	14
5.2	Interpretation as a topological obstruction	16
6	Conclusion	17
	References	18

1 Introduction

The use of color exchange was introduced a long time ago by Kempe in its attempt to prove that four colors were always sufficient to color a planar graph [1]. It was later realized that such exchanges of colors cannot be used in general to reach all possible colorings of a graph: colorings form equivalence classes and there are obstructions to connect them [2]. The same issue appeared, more recently, in the physics of magnetism where dynamics of colors (that of spins) consist precisely of exchange transformations [3,4]. The existence of classes of states, or “Kempe sectors”, makes the physical dynamics nonergodic and it is a question to understand the obstructions and, possibly, to compute the invariants of the dynamics, which are characteristic of each class. The subject is at the frontier of discrete mathematics which have studied under which conditions the “reconfiguration graph” is connected [5,6], and loop dynamics or gauge theories in physics, where ergodicity issues are particularly important, not only for technical reasons, as in Monte Carlo sampling [3], but also in connection with glassy dynamics and conservation laws.

The coloring of the edges of the regular hexagonal lattice with three colors [7] appears as a very simple physical model that could describe some antiferromagnetic materials (the three colors being three spins at 120°), where the absence of ergodicity [3,4,8] can be studied in details. Similar problems have been raised in two-color (dimer) models in three-dimensional lattices [9,10], and seem therefore to be quite a general issue. Concerning the problem of the hexagonal lattice, a first invariant has been found [11,12] and describes two (odd/even) classes of states, which are both extensive with system size [13]. This first invariant can be seen, mathematically, as the parity of the *degree* of a color map [14]. We recently argued that a complete classification of the sectors can be obtained by additional stable invariants [15]. This needs to put aside the vast majority of sectors that result from steric constraints [15].

Such coloring satisfaction problems reveal 2-colored subregions, called “Kempe chains”, surrounded by other colors, within which the colors can be exchanged. On certain lattices, Kempe chains have the form of closed loops (that can be viewed as flux lines through a line in 2 dimensions). Since the loops evolve under the dynamics, it is natural to consider them up to some deformations, *i.e.* up to *homotopies*, and see them as elements of the fundamental group of the surface on which the lattice is defined. For example, on a lattice with periodic boundary conditions, *i.e.* a torus shape, that we will consider hereafter, the loops are characterized by their winding numbers -also called “fluxes”. Individual winding numbers are not conserved but it appeared that some polynomials of the winding numbers are conserved, these are the invariants mentioned above [15].

This raises the following question which we address in the present paper. While, for example, standard vortices are characterized by their (integer) vorticity -or elements of the first homotopy group-, is it possible to provide a similar topological interpretation of such color invariants? Is there a known obstruction characterized by homotopy group elements? We will see that the *linking* numbers of the Kempe loops are the natural numbers to visualize some of these invariants. However, since linking numbers are defined in three, not in two, dimensions, it is necessary to visualize the surface on which the lattice is defined in three dimensions and there are several inequivalent ways to do it [16]. Note that, in the dynamical evolution, the loops can cross and be subject to “surgeries”, with cutting and reconnections, so that there is no guarantee that linking numbers will be conserved in any way.

To study this question, we will consider two types of dynamics, the dynamics originally

considered in Ref. [15], directly motivated by the color problem, which we call “dynamics I” here in section 2.1, and a modified dynamics (with an additional constraint), “dynamics II” in section 2.2. We will give the invariants of both dynamics in section 2. In section 3.1, we will see that a color invariant of “dynamics II” is directly interpreted as linking numbers on the *standard torus in 3d*. This surface has to be modified for “dynamics I” in terms of special surfaces with self-intersections, *i.e. immersions* in 3d. We will explain how to define the linking numbers, first on a simple instance of immersion in section 3.2, and, second, on general immersions in section 3.3. In what sense such linking numbers are topological invariants of surfaces is explained in section 3.4. In section 4, we discuss the two equivalence classes of torus immersions, and, in section 5 why we need a special immersion to interpret the invariant of “dynamics I”, and why the color invariant reflects the obstruction to transform the corresponding immersion into its chiral image.

2 Invariants of 2d flux lines dynamics

2.1 Dynamics I

The model consists of coloring the edges of the 2d hexagonal lattice with three colors A, B, and C [7]. It is then possible to define three types of loops of edges A-B, A-C and B-C, called “Kempe” chains. On a lattice with periodic boundary conditions (*i.e.* it is defined on a torus T^2), such a loop is always closed and has two integer winding numbers (p, q) that characterize how many times it winds around the boundaries. It can be seen, up to homotopy, as an element of the fundamental group of the torus, $\pi_1(T^2) = \mathbb{Z} \times \mathbb{Z}$.

A color configuration is thus characterized by a triplet of integer vectors, $(\mathbf{a}, \mathbf{b}, \mathbf{c})$, where $\mathbf{a} = (a_x, a_y)$ defines the two total integer winding numbers (or “fluxes”) of all B-C loops, $\mathbf{b} = (b_x, b_y)$ for the C-A loops and $\mathbf{c} = (c_x, c_y)$ for the A-B loops (we will sometimes use a third component a_z defined by $a_z \equiv -a_x - a_y$). The triplet of vectors $(\mathbf{a}, \mathbf{b}, \mathbf{c})$ satisfies the equation [15],

$$\mathbf{a} + \mathbf{b} + \mathbf{c} = 0, \quad (1)$$

showing that there are four independent integers, *e.g.* (a_x, a_y, b_x, b_y) . Color exchanges correspond to exchanging the two colors B and C of a closed loop of type a , or C and A for type b or A and B for type c , resulting in three possible transformations of integer vectors $(\mathbf{a}, \mathbf{b}, \mathbf{c})$ to $(\mathbf{a}', \mathbf{b}', \mathbf{c}')$, as follows [15],

$$(\mathbf{a}', \mathbf{b}', \mathbf{c}') = (\mathbf{a} + 2k\hat{\mathbf{a}}, \mathbf{b} - k\hat{\mathbf{a}}, \mathbf{c} - k\hat{\mathbf{a}}), \quad (2)$$

$$(\mathbf{a}', \mathbf{b}', \mathbf{c}') = (\mathbf{a} - k\hat{\mathbf{b}}, \mathbf{b} + 2k\hat{\mathbf{b}}, \mathbf{c} - k\hat{\mathbf{b}}), \quad (3)$$

$$(\mathbf{a}', \mathbf{b}', \mathbf{c}') = (\mathbf{a} - k\hat{\mathbf{c}}, \mathbf{b} - k\hat{\mathbf{c}}, \mathbf{c} + 2k\hat{\mathbf{c}}), \quad (4)$$

where $\hat{\mathbf{a}} = \frac{\mathbf{a}}{\text{gcd}(a_x, a_y)}$ is a *primitive* vector along \mathbf{a} , $\text{gcd}(a_x, a_y)$ is the greatest common divisor of a_x and a_y and is basically the number of disconnected winding loops of type a . The positive or negative integer k gives the possibility to insert pairs of parallel winding loops or flip them. Since $\mathbf{a}, \mathbf{b}, \mathbf{c}$ play the same role, it is possible to permute them (up to a change of sign) by a suitable choice of k .

The integer dynamics described by Eqs.(2)-(4) is subject to several constraints which originate in the coloring problem [15]. The first constraint is a steric constraint; the lattice

has finite linear size L and there is a maximal packing of winding loops, giving necessarily,

$$|a_\alpha| \leq L, \quad |b_\alpha| \leq L, \quad |c_\alpha| \leq L, \quad (5)$$

where $\alpha = x, y$ or z . The four independent integers therefore evolve inside a “box”, $[-L, L]^4$. The second constraint arises from the interpretation of loops as colors, and takes the form of linear constraints,

$$\mathbf{a} - \mathbf{b} = \mathbf{L} \pmod{3}, \quad (6)$$

$$\mathbf{c} - \mathbf{a} = \mathbf{L} \pmod{3}, \quad (7)$$

$$\mathbf{b} - \mathbf{c} = \mathbf{L} \pmod{3}, \quad (8)$$

where \mathbf{L} is a notation for (L, L) . Not all sets of four independent integers (a_x, b_x, a_y, b_y) are therefore allowed and the constraints can be seen as partitioning the box in sectors characterized by $L \pmod{3}$. Such constraints *e.g.* $\mathbf{a}' - \mathbf{b}' = \mathbf{a} - \mathbf{b} + 3k\hat{\mathbf{a}}$, are naturally conserved, modulo 3, by the dynamics. What is remarkable is that these sectors split into subsectors. The problem is to classify equivalent classes of triplets $(\mathbf{a}, \mathbf{b}, \mathbf{c})$ up to the transformations given by Eqs. (2)-(4).

We have several invariants [15], which we recall,

$$I_0 = \mathbf{a} + \mathbf{b} + \mathbf{c}, \quad (9)$$

$$I_1 = \frac{1}{3}(\mathbf{a} \times \mathbf{b} + \mathbf{b} \times \mathbf{c} + \mathbf{c} \times \mathbf{a}) \pmod{2}. \quad (10)$$

$I_0 = 0$ for the physical color problem. The case $I_1 = 0$ corresponds to a connected “even” sector. The case $I_1 = 1$ corresponds to the “odd” sectors, which have two additional invariants,

$$I_2 = \frac{1}{3}(\mathbf{a} \cdot \mathbf{b} + \mathbf{b} \cdot \mathbf{c} + \mathbf{c} \cdot \mathbf{a}) \pmod{4}, \quad (11)$$

$$I_3^\pm = P_5^\pm(\mathbf{a}, \mathbf{b}, \mathbf{c}) \pmod{4}, \quad (12)$$

where $I_2 = \pm 1$ and $I_3^\pm = \pm 1$ (meant modulo 4) and the upper script \pm means for the corresponding value of $I_2 = \pm 1$. $P_5^\pm(\mathbf{a}, \mathbf{b}, \mathbf{c})$ is a polynomial of degree 5 (symmetrical under the permutations of \mathbf{a} , \mathbf{b} and \mathbf{c}) [15]. We thus have 5 sectors: a connected sector with $I_1 = 0$ (even sector) and 4 sectors for $I_1 = 1$ (odd sectors), fully described by $I_2 = \pm 1$ and $I_3^\pm = \pm 1$. Additional sectors exist, but are “unstable” when the “box” constraints given by Eq. 5 are relaxed to $L_1 \geq L$. These sectors get reconnected through higher winding number configurations and are thus not related to a stable invariant. The set I_0, I_1, I_2 and I_3^\pm was argued to be a complete set of stable invariants for dynamics I [15].

While I_1 has a simple interpretation in terms of the parity of the number of signed crossings of winding loops, we will be interested here in interpreting I_2 , and leave the interpretation of I_3^\pm as an open question.

Since by permutation, it is always possible to consider configurations with a given parity of the winding numbers, $(\mathbf{a}, \mathbf{b}, \mathbf{c}) \pmod{2}$, for example $(1, 0, 1, 0, 1, 1, 1, 1, 0)$ (one of the six possibilities in an odd sector), we can rewrite I_2 as

$$I_2 = 2(a_x b_x + a_y b_y) + a_x b_y + a_y b_x \pmod{4}. \quad (13)$$

This is under this form that we will interpret I_2 as a linking number of a and b curves on a special immersion (section 5).

2.2 Dynamics II

We now include an additional constraint, a “parity control” to the previous dynamics. We will show numerically that the sectors split into 23 stable sectors (instead of 16 if there were no new nontrivial sectors as we will see below) and will give the invariants explicitly.

The additional constraints we consider are

$$a'_x = a_x \pmod{2}, \quad (14)$$

$$b'_x = b_x \pmod{2}, \quad (15)$$

$$c'_x = c_x \pmod{2}, \quad (16)$$

where a'_x is the x -component of \mathbf{a}' (after a color exchange). We thus impose a “parity control” on

$$P = (a_x, b_x, c_x) \pmod{2}, \quad (17)$$

which the dynamics II must conserve.

The previous invariants still hold, since the dynamical equations are the same and we can consider, in particular, even sectors ($I_1 = 0$) and odd sectors ($I_1 = 1$).

We have numerically iterated the dynamics, $(\mathbf{a}, \mathbf{b}, \mathbf{c}) \rightarrow (\mathbf{a}', \mathbf{b}', \mathbf{c}')$ [Eqs. (2)-(4)] under all previous and current constraints, *i.e.* by rejecting the moves that do not satisfy the constraints. We use a numerical depth-first search algorithm, which terminates once all states connected to an initial state are exhausted and thus construct the sectors.

We find that the even sector ($I_1 = 0$), which was *connected* in dynamics I, now splits into many subsectors. In Fig. 1, we give the result of the distribution of sizes of each even Kempe sector up to $L = 100$. We find a very large number of small sectors (containing typically less than L configurations) and 11 large sectors. Some have symmetries as seen in the degeneracies: six sectors, on one hand, have the same size, and there are two doublet sectors).

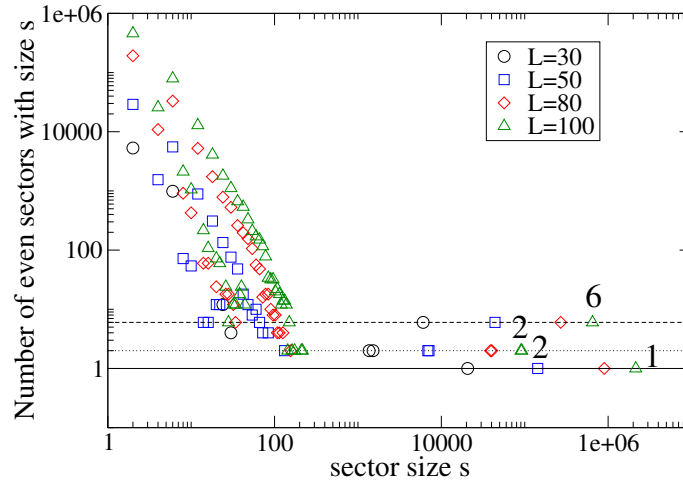


Figure 1: Distribution of sizes of even sectors of dynamics II for various linear sizes L (logarithmic scales). We note a numerous number of small sectors and 11 large sectors, with a clear separation between the two.

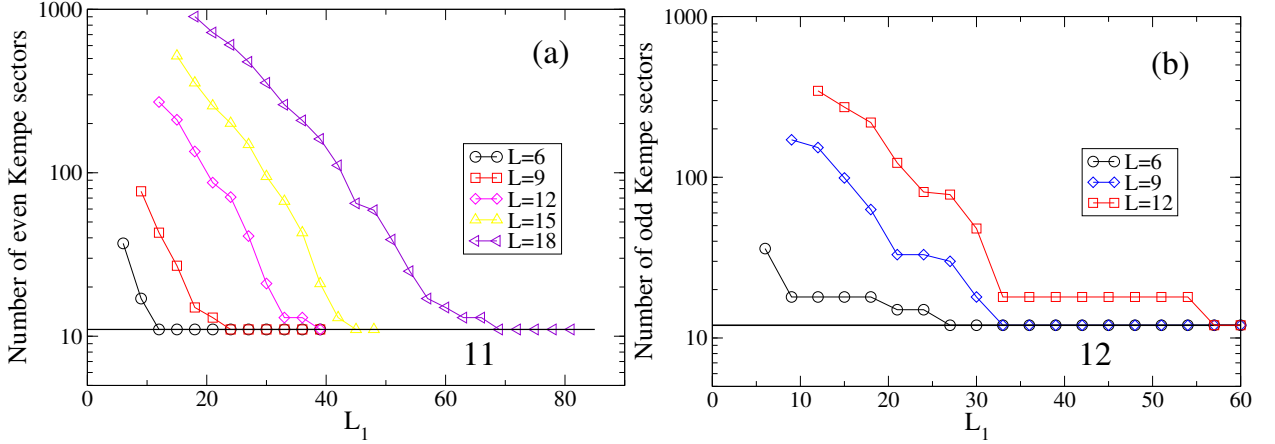


Figure 2: Stabilization of the number of even (a) and odd (b) sectors. The two numbers 11 and 12 give the number of stable sectors (invariant-related).

In Fig. 2, we study the convergence of the number of sectors when the “box” constraints given by Eq. 5 are progressively relaxed by allowing intermediate configurations with winding numbers up to $L_1 \geq L$. It gives the convergence of the number of sectors with size: 11 even sectors and 12 odd sectors and reflects the reconnections of the smaller sectors, which, as we argued earlier [15], are not related to stable invariants.

In order to study the stable invariants, we generate only the configurations that belong to the large sectors, by introducing a size cutoff, typically a few L (as found in Fig. 1). In this way, we can study the regularities in the winding numbers and extract the stable invariants.

We can first consider sectors according to their conserved parity P . Among the $2^3 = 8$ possibilities for P , we have only 4 since $a_x + b_x + c_x = 0$: $P = (0, 0, 0); (0, 1, 1); (1, 0, 1); (1, 1, 0)$.

In the even sector, all four possibilities,

$$P = (0, 0, 0); (0, 1, 1); (1, 0, 1); (1, 1, 0), \quad (18)$$

are compatible with even $\chi = a_x b_y - a_y b_x$, giving four trivial sectors. In fact, the sector $P = (0, 0, 0)$ splits into 5 sectors, see Table 1, and the three others split into 2 sectors, so that we get the 11 sectors of the even sector (as found in Fig. 1 and Fig. 2 (a)).

In the odd sector, there remains only three possibilities among four,

$$P = (0, 1, 1); (1, 0, 1); (1, 1, 0), \quad (19)$$

because $(0, 0, 0)$ is not compatible with an odd χ . Since each of the three must be split into four, according to the invariants described in section 2.1, this simply explains the 12 odd sectors observed. It shows that there are no additional nontrivial sectors and invariants in the odd sector. We now describe the nontrivial sectors of the even sector.

2.2.1 Additional invariants of the even sector.

Among the four possibilities of parity control (18), consider first $P = (0, 1, 1), (1, 0, 1)$ or $(1, 1, 0)$. We have found numerically that

$$I'_2 = \frac{a_x b_y + a_y b_x + b_x c_y + b_y c_x + c_x a_y + c_y a_x}{2} \pmod{2} \quad (20)$$

		Sect.	P	I_2'	I_2''	$I_3^{\pm'}$	$(\mathbf{a}, \mathbf{b}, \mathbf{c})$	n^2
$L = 0 \pmod{3}$	1	(0,0,0)	0	-	-		0	0
	2	(0,0,0)	1	1	-1		(2, -2, 0, 2, 1, -3, -4, 1, 3)	8
	3	(0,0,0)	1	1	1		(-2, -2, 0, 2, 1, -3, -4, 1, 3)	8
	4	(0,0,0)	1	-1	-1		(-2, 0, -2, 2, -3, 1, -4, 3, 1)	8
	5	(0,0,0)	1	-1	1		(2, 0, -2, 2, -3, 1, -4, 3, 1)	8
	6	(0,1,1)	0	-	-		$\pm(2, 0, -2, -1, 0, 1, -1, 0, 1)$	2
	7	(0,1,1)	1	-	-		$\pm(2, -2, 0, -1, 1, 0, -1, 1, 0)$	2
	8	(1,0,1)	0	-	-		$\pm(-1, 0, 1, 2, 0, -2, -1, 0, 1)$	2
	9	(1,0,1)	1	-	-		$\pm(-1, 1, 0, 2, -2, 0, -1, 1, 0)$	2
	10	(1,1,0)	0	-	-		$\pm(-1, 0, 1, -1, 0, 1, 2, 0, -2)$	2
	11	(1,1,0)	1	-	-		$\pm(-1, 1, 0, -1, 1, 0, 2, -2, 0)$	2
		Sect.	P	I_2'	I_2''	$I_3^{\pm'}$	$(\mathbf{a}, \mathbf{b}, \mathbf{c})$	n^2
$L = 1 \pmod{3}$	1	(0,0,0)	0	-	-		(0, 0, 0, 2, -1, -1, -2, 1, 1)	2
	2	(0,0,0)	1	1	-1		(2, -2, 0, 4, -3, -1, -6, 5, 1)	16
	3	(0,0,0)	1	1	1		(2, 0, -2, -2, -1, 3, 0, 1, -1)	4
	4	(0,0,0)	1	-1	-1		(2, -2, 0, -2, 3, -1, 0, -1, 1)	4
	5	(0,0,0)	1	-1	1		(2, 0, -2, 4, -1, -3, -6, 1, 5)	16
	6	(0,1,1)	0	-	-		(0, 0, 0, -1, 2, -1, 1, -2, 1)	2
	7	(0,1,1)	1	-	-		(0, 0, 0, -1, -1, 2, 1, 1, -2)	2
	8	(1,0,1)	0	-	-		(-1, 2, -1, 0, 0, 0, 1, -2, 1)	2
	9	(1,0,1)	1	-	-		(-1, -1, 2, 0, 0, 0, 1, 1, -2)	2
	10	(1,1,0)	0	-	-		(-1, 2, -1, 1, -2, 1, 0, 0, 0)	2
	11	(1,1,0)	1	-	-		(-1, -1, 2, 1, 1, -2, 0, 0, 0)	2

Table 1: The splitting of the even sector ($I_1 = 0$) into 11 subsectors conserved by dynamics Π and classified by the imposed “parity control” P and the nontrivial invariants $I_2', I_2'', I_3^{\pm'}$, for $L = 0, 1 \pmod{3}$ (for $L = 2 \pmod{3}$, change all signs in $(\mathbf{a}, \mathbf{b}, \mathbf{c})$ of $L = 1 \pmod{3}$). Examples of configurations $(\mathbf{a}, \mathbf{b}, \mathbf{c})$, (with the smallest norm $n^2 = \frac{1}{6} \sum_{i=x,y,z} (a_i^2 + b_i^2 + c_i^2)$) are given.

is invariant in the dynamics II (when $I_1 = 0$). In this expression, there are always four terms that cancel. For example, for $P = (0, 1, 1)$,

$$I_2' = \frac{b_x c_y + b_y c_x}{2} \pmod{2}. \quad (21)$$

Indeed, since $I_1 = 0$, $a_x b_y - a_y b_x$ is even, a_x is even so $a_x b_y$ is even. b_x is odd so a_y must be even. Since $a_x + a_y + a_z = 0$, one must have a_z even. Therefore $\mathbf{a} \pmod{2} = 0$. We see that $(a_x b_y + a_x c_y)/2 = a_x(b_y + c_y)/2 = -a_x a_y/2$ is an integer multiple of two. The same argument applies to $(a_y b_x + a_y c_x)/2$.

Second, consider $P = (0, 0, 0)$. Since, by definition, a_x, b_x and c_x are even, define,

$$\tilde{\mathbf{a}} = (a_x/2, a_y, -a_x/2 - a_y), \quad (22)$$

$$\tilde{\mathbf{b}} = (b_x/2, b_y, -b_x/2 - b_y), \quad (23)$$

$$\tilde{\mathbf{c}} = (c_x/2, c_y, -c_x/2 - c_y). \quad (24)$$

They are all integer numbers and all constraints are satisfied, $\tilde{\mathbf{a}} + \tilde{\mathbf{b}} + \tilde{\mathbf{c}} = 0$, $\tilde{a}_x + \tilde{a}_y + \tilde{a}_z = 0$ *etc.* We also have

$$\tilde{a}_x \tilde{b}_y - \tilde{a}_y \tilde{b}_x = \chi/2 = 1 + 2n = 1 \pmod{2}, \quad (25)$$

so that $(\tilde{\mathbf{a}}, \tilde{\mathbf{b}}, \tilde{\mathbf{c}})$ is a valid state in an odd sector. We can therefore label it by I_2 and I_3^\pm of section 2.1. We can apply the dynamics to $(\tilde{\mathbf{a}}, \tilde{\mathbf{b}}, \tilde{\mathbf{c}})$ and generate a new state $(\tilde{\mathbf{a}}', \tilde{\mathbf{b}}', \tilde{\mathbf{c}}')$. Then, by inverting the linear transformation above, we have a new state $(\mathbf{a}', \mathbf{b}', \mathbf{c}')$ which is in the same sector as $(\mathbf{a}, \mathbf{b}, \mathbf{c})$, labeled by the same invariants. Knowing the invariants for odd sectors [Eq. 11], we generate new invariants for the even sectors:

$$I_2'' = \frac{1}{3}(\tilde{\mathbf{a}} \cdot \tilde{\mathbf{b}} + \tilde{\mathbf{b}} \cdot \tilde{\mathbf{c}} + \tilde{\mathbf{c}} \cdot \tilde{\mathbf{a}}) \pmod{4}, \quad (26)$$

the three terms giving equal contribution. We replace and obtain

$$\tilde{\mathbf{a}} \cdot \tilde{\mathbf{b}} = \frac{a_x b_x}{2} + 2a_y b_y + \frac{1}{2}(a_x b_y + a_y b_x). \quad (27)$$

By noticing that,

$$\frac{1}{3} \left[\frac{1}{2}(a_x b_x + b_x c_x + c_x a_x) + 2(a_y b_y + b_y c_y + c_y a_y) \right] \quad (28)$$

vanishes modulo 4 in these sectors, I_2'' simplifies:

$$I_2'' = \frac{1}{6}(a_x b_y + a_y b_x + b_x c_y + b_y c_x + c_x a_y + c_y a_x) \pmod{4}. \quad (29)$$

Similarly, we define, $I_3^\pm(\mathbf{a}, \mathbf{b}, \mathbf{c}) = P_5^\pm(\tilde{\mathbf{a}}, \tilde{\mathbf{b}}, \tilde{\mathbf{c}}) \pmod{4}$, where P_5^\pm is the corresponding invariant of dynamics I.

The integer numbers P , I_2' , I_2'' and $I_3^{\pm'}$ give a complete classification of the 11 stable even sectors ($I_1 = 0$) of dynamics II, while P , I_2 , and I_3^\pm give a complete classification of the 12 stable odd sectors ($I_1 = 1$).

3 Definition of the linking number

The linking number of two curves in 3d space is defined, as usual, as the number of signed intersections of one curve with the surface whose boundary is the second curve, called a Seifert surface.

When two curves have intersection points, there is an ambiguity in the definition of the linking number. We generally average over all possible resolutions of the intersections, by shifting one of the two curves in the two possible ways away from the intersection point. This extends the linking numbers to half-integer values, the half-integer part representing the number of intersection points.

3.1 Linking number on the standard torus in 3d

The linking number for arbitrary curves on the embedded (with no self-intersection) torus in 3d is defined as a bilinear form of the cycles. It depends only on the homology class and not on the cycles themselves. Consider a cycle as a vector in a vector space $(H_1(T^2, \mathbb{Z}))$, the first homology group with coefficients in \mathbb{Z} , which can be written

$$\mathbf{a} = a_x \mathbf{x} + a_y \mathbf{y} \quad (30)$$

where \mathbf{x} and \mathbf{y} are two basis cycles and a_x, a_y the two integer winding numbers. Then, the linking number of \mathbf{a} and \mathbf{b} is defined as

$$lk(\mathbf{a}, \mathbf{b}) = a_x b_x lk(\mathbf{x}, \mathbf{x}) + a_x b_y lk(\mathbf{x}, \mathbf{y}) + a_y b_x lk(\mathbf{y}, \mathbf{x}) + a_y b_y lk(\mathbf{y}, \mathbf{y}). \quad (31)$$

Note that $lk(\mathbf{x}, \mathbf{x}) = lk(\mathbf{y}, \mathbf{y}) = 0$ and $lk(\mathbf{x}, \mathbf{y}) = lk(\mathbf{y}, \mathbf{x}) = 1/2$, since the cycles \mathbf{x} and \mathbf{y} have one intersection point, so that

$$lk(\mathbf{a}, \mathbf{b}) = \frac{1}{2}(a_x b_y + a_y b_x). \quad (32)$$

For example, the curve that corresponds to the cycle $\mathbf{a} = (1, 1)$ has $lk(\mathbf{a}, \mathbf{a}) = 1$, it is “self-linked”, or is a “torus knot”.

This form, Eq. (32), of the linking number actually corresponds to the invariant I_2'' of the dynamics II, Eq. (20), and is, therefore, conserved by dynamics II. It appears now as obvious that sectors 6 and 7 for instance (see table 1), with, respectively, $I_2' = 0$ and $I_2' = 1$, can be seen as two unlinked (resp. linked), loops. In sector 6, the configuration with $\mathbf{b} = (1, 0)$ and $\mathbf{c} = (1, 0)$ are two parallel unlinked loops, $lk(\mathbf{b}, \mathbf{c}) = 0$. In sector 7, $\mathbf{b} = (1, -1)$ and $\mathbf{c} = (1, -1)$ are two parallel linked loops, $lk(\mathbf{b}, \mathbf{c}) = 1$. Since the invariant is conserved only modulo 2, there is no higher linking number. The obstruction characterized by I_2' therefore simply corresponds to the impossibility to dynamically unlink the two loops.

In sectors with $P = (0, 0, 0)$, the conservation of I_2'' can also be expressed in terms of linking numbers. From Eq. (29),

$$I_2'' = \frac{1}{3} [lk(\mathbf{a}, \mathbf{b}) + lk(\mathbf{b}, \mathbf{c}) + lk(\mathbf{c}, \mathbf{a})] \pmod{4}, \quad (33)$$

and the same interpretation holds, modulo 4.

In order to describe other invariants such as I_2 , it is necessary to modify the expression of the linking form, Eq. (32) and change the linking properties of the basis cycles, *e.g.* $lk(\mathbf{x}, \mathbf{x})$, in Eq. (31). As we will see, this results in surfaces with self-intersections in 3d, *i.e.* *immersions*.

3.2 Linking number on the double cover of the torus

We consider here the simplest example of an immersion of a torus to explain why, in general, the linking number on immersions is *ill-defined*. The linking number of two curves will indeed depend on the relative positions of them and when one of them is deformed (evolves dynamically), the linking number will change. To understand this point, consider the immersion shown in Fig. 3 (b). It is a double cover of the torus obtained by identifying the edges of the surface (Fig. 3 (a)) and mapping the two curves Δ_1 and Δ_2 on Δ , which becomes a self-intersection curve in 3d.

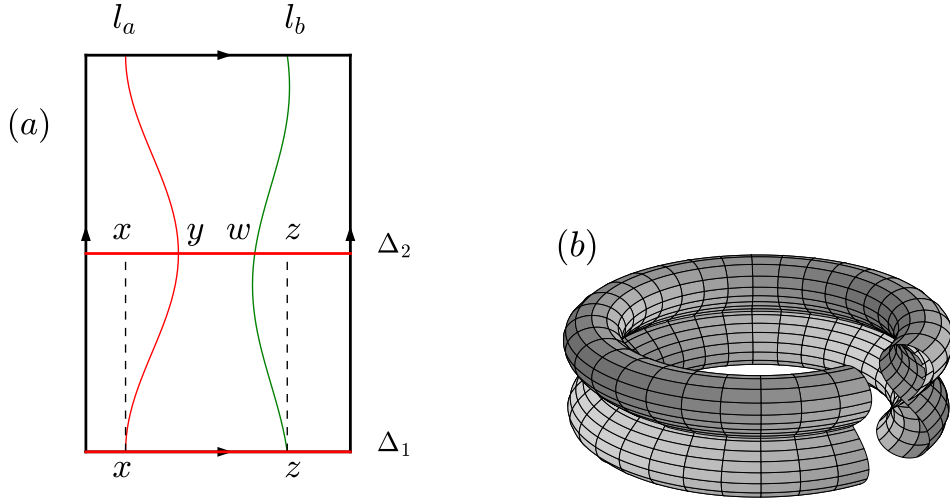


Figure 3: A surface with the topology of a torus, with the identification of Δ_1 and Δ_2 and the edges (a), which is a double cover of the torus over a parallel Δ_1 . Two arbitrary closed loops l_a and l_b are represented. An immersion of it in 3d is shown in (b), with its self-intersection curve Δ , with preimages Δ_1 and Δ_2 .

Consider, in Fig. 3 (a), a first closed loop l_a which cuts Δ_1 in x and Δ_2 in y and a second loop l_b which cuts them in w and z . When l_a moves in its homotopy class, the point y of l_a , in particular, will move on Δ_2 and may cross the point z of l_b : it gives an intersection point of the corresponding curves L_a and L_b on the immersion in 3d, and, hence, a jump of the linking number by ± 1 (depending on the orientation).

We say that the couple of points (y, z) are “ordered” if they occur in this order on Δ and introduce a number $\sharp(l_a, l_b) = 0$ in this case. If y crosses over z , (z, y) are “disordered” by a single permutation, so that we define $\sharp(l_a, l_b) = 1$ to compensate the jump of the linking number. We see also that moving homotopically l_a to the left in Fig. 3 (a) and crossing the boundary will permute y and z : the couples (y, z) and (z, y) are physically equivalent, or in other words, $\sharp(l_a, l_b)$ is defined only modulo 1.

In this case, the linking number itself is defined only modulo 1. Since it can be a half-integer or an integer, it does not reflect anything else than the parity of crossings.

3.3 Linking number on an arbitrary immersion of the torus

We now consider an arbitrary immersion of the torus in 3d. Its self-intersection curve Δ is characterized by its winding numbers. To define them with sign, it is necessary to give an orientation to Δ . For a point x in Δ , we define two vectors ξ_1 and ξ_2 , ξ_i being normal to the sheet containing the two preimages Δ_i ($i = 1, 2$). Unless the two sheets are parallel (which does not happen generically), the orientation e is unambiguously defined by $\xi_1 \times \xi_2$. Note that we can consider that this is the orientation of Δ_1 (while that of Δ_2 will be opposite).

With this orientation, if the self-intersection curve Δ is connected, its winding numbers are noted $\delta = (\delta_x, \delta_y)$ where δ_x and δ_y are positive or negative integers. Suppose that the two components of

$$\delta = (nq, mq), \quad (34)$$

are multiples of q , the greatest common divisor, $q = \text{gcd}(\delta_x, \delta_y) > 0$. In this case, we shall say that the immersion is “ q -perfect”. For example, with this definition, the double covered torus (previous paragraph) is “1-perfect” since its connected self-intersection curve has winding numbers $(1, 0)$, $q = 1$.

More generally, if the self-intersection curve Δ is *not* connected and has m components, the integer q is defined as the greatest common divisor of the set of all winding numbers,

$$(\delta_x^1, \delta_y^1, \dots, \delta_x^m, \delta_y^m). \quad (35)$$

This is the most general definition of a “ q -perfect” immersion. If the set is empty or if all the winding numbers are zero, we say that the immersion is “ ∞ -perfect”. Note that an immersion that is 6-perfect, for example, is also 2 and 3-perfect but the converse, is of course, not true.

As a consequence of this definition, a loop l_a with winding numbers \mathbf{a} will have $\mathbf{a} \times \delta$ signed crossings with the self-intersection curve, which will be a multiple of q . The loop l_a crosses Δ_1 in a certain number of points, x_1, \dots, x_s , each equipped with a sign (because l_a and Δ_1 are orientated). Similarly, a second loop l_b crosses Δ_2 in y_1, \dots, y_r . These points correspond to some points on Δ_1 , which are sent to the same points on Δ by the immersion. If l_a passes through one of these points on Δ_1 , there will be an intersection of l_a and l_b on Δ . We can first consider that l_a avoids these points so that the x 's and y 's are placed in some order, going along Δ_1 . One can define some particular order, *e.g.* all the x 's to the left of all the y 's (or it can be empty), and call it the “normal order”, for which we have (by definition) a “disorder” number,

$$\#(l_a, l_b) = 0. \quad (36)$$

Now for a generic configuration, the disorder number $\#(l_a, l_b)$ is defined as the signed number of permutations of the x 's and y 's. Because of the torus geometry, one can move l_a to the right of the set y_1, \dots, y_r to realize a different order. This corresponds to a certain number of permutations of the normal order, that is a multiple of q ,

$$\#(l_a, l_b) = nq, n \in \mathbb{Z}. \quad (37)$$

However, it is the same state as the original one, so to match the disorder numbers, we have to define it modulo q ,

$$\#(l_a, l_b) = 0 \pmod{q}. \quad (38)$$

Now each crossing of l_a with a point y_j permutes the order by a transposition, $x_i y_j \rightarrow y_j x_i$, it corresponds to a crossing of the two lines l_a and l_b on the immersion and a jump of the linking number, which we correct by counting the permutation, $\#(l_a, l_b) = \pm 1 \pmod{q}$.

Consider the linking number,

$$LK(\mathbf{a}, \mathbf{b}) = lk(L_a, L_b) + \sharp(l_a, l_b) \pmod{q}, \quad (39)$$

which is a half-integer number: \mathbf{a} labels the homotopy class of l_a (the closed loop on the surface), whereas L_a is its image on the immersion. It is now a well-defined integer modulo q for a q -perfect immersion, that depends only on the homotopy classes of the loops, not the loops themselves. If the immersion is ∞ -perfect, the linking number is well-defined for any q , in particular for an embedding for which $\sharp(l_a, l_b) = 0$ and the expression reduces to the standard linking number.

3.4 A topological invariant

We now explain that the integer linking number given by Eq. (39) is a topological invariant of the immersed surface. We call two immersions φ_1 and φ_2 “ q -perfect regular homotopic” if there exists a regular [19] homotopy φ_t with $t \in [0, 1]$, which coincides with the two immersions at $t = 0$ and $t = 1$, and such that an arbitrary immersion φ_t is q -perfect. In other words, the deformation of the initial immersion should be such that the self-intersection curve remains q -perfect at all “times”. In this case, the half-integer linking number (39) is a topological invariant. The existence of different immersions for which it is possible to compute the topological invariant given by Eq. 39 will tell us, if these numbers differ, that there is no q -perfect regular homotopy between them, and thus gives us some information on the evolution of the winding properties of the self-intersection curve upon regular homotopy. We now consider the example of the torus.

4 Two classes of immersed torus

We now consider immersions of the torus in 3d, up to regular homotopies and reparametrizations: it is known [17] that there are two classes of immersed torus (contrary to the single regular homotopy class of the 2-spheres), a representative of each is shown in Fig. 4 and will be described below. The regular homotopies conserve an invariant, which is called the Arf-Kervaire invariant of the immersion s ,

$$Arf(s) = q(x)q(y) \pmod{2}, \quad (40)$$

where x and y are two independent cycles on the surface and the function $q(x)$ is defined as follows. $q(x)$ measures the integer number of 2π -turns of a “thickened” cycle x (also called the “tubular neighbourhood” or x). A “thickened” cycle is an infinitesimal “ribbon” constructed on the surface with x as one edge and a parallel copy of x as the second edge. The “ribbon” has a well-defined frame, a collection of three orthogonal unit vectors that measures its local orientation (tangent to the cycle, normal to it and belonging to the surface, and binormal, *i.e.* perpendicular to the surface). The frame defines at each point of the ribbon an $SO(3)$ matrix which is obtained by rotating a reference frame onto the local frame thus defined. In turn, this defines a continuous application from the cycle S^1 onto $SO(3)$. We know that there are two homotopy classes of such maps corresponding to $\pi_1[SO(3)] = \mathbb{Z}_2$: the generator corresponds to the Frenet-Serret frame of the simple circle. When thickened, it gives an untwisted ribbon with $q(x) = 0$. The trivial element on the other hand is the circle run over twice, or, as a ribbon, the twisted ribbon (by a 2π -turn); *i.e.* $q(x) = 1$.

An alternative viewpoint is to consider the two edges of the ribbon, one is the original cycle x and the other one is its “parallel” copy, x' . It is easy to see that when the ribbon is twisted by a 2π -turn, its two edges x and x' are linked with linking coefficient $lk(x, x') = \pm 1$ (with a sign depending on the orientation). Whereas when the ribbon makes no turn, the two cycles are obviously unlinked and $lk(x, x') = 0$. So that we can also define

$$q(x) = lk(x, x'), \quad (41)$$

and $q(x)$ is either 0 or 1 by definition. We have therefore two types of ribbons that we cannot continuously deform into each other. They allow to define two inequivalent immersed torus, characterized by the Arf-Kervaire invariant, Eq. (40), that cannot be connected by regular homotopy [17].

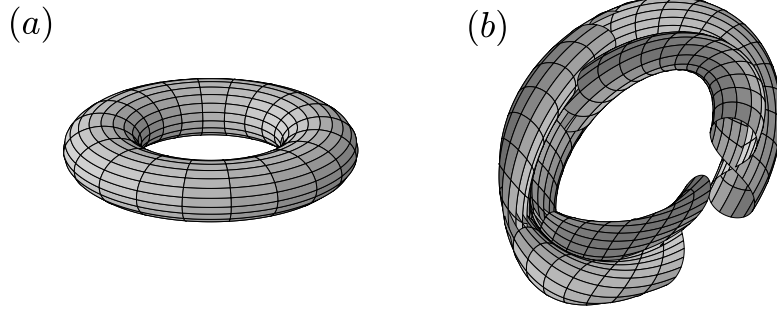


Figure 4: Two inequivalent classes of immersed torus up to regular homotopies: (a) standard, embedded, Arf-Kervaire 0, torus; (b) immersion, Arf-Kervaire 1, self-linked torus, which is similar to that of Fig. 3 with a twist.

The first torus [Fig. 4 (a)] is the *standard* embedded torus in 3d. It has two cycles x and y which satisfy $q(x) = q(y) = 0$, which means that the two corresponding ribbons are untwisted (or their edges unlinked): it has an Arf-Kervaire invariant of zero.

The second torus [Fig. 4 (b)] has two cycles x and y which satisfy $q(x) = q(y) = 1$, so that the two ribbons are twisted, and we say that the cycles are “self-linked”. It has an Arf-Kervaire invariant of one. The simplest example of such a torus consists of rotating a lemniscate (a planar curve with the shape of the number eight) by 2π while moving its double point along a closed circle. This generates a torus which is immersed in space, with a self-intersection line which originates in the double point of the lemniscate. The first cycle x consists of following a single lemniscate, avoiding its double point. The corresponding thickened cycle is twisted by 2π . The second cycle y consists of following a point at the top of the lemniscate while rotating it, it is equivalent to a $(1, 1)$ cycle on a regular torus and hence is “self-linked”. This is therefore an example of an immersed torus with Arf-Kervaire invariant one. The self-intersection curve has winding numbers $(1, 0)$, in this instance (the immersion is 1-perfect). In the following, we will need to construct a variant of this surface with a self-intersection curve that has no such winding components.

It is also known that the Arf-Kervaire invariant is not only a homotopy invariant but also a regular cobordism invariant, and hence an invariant of higher homotopy groups [20]. A consequence is that the present immersion represents the nontrivial element of the stable homotopy group $\Pi_2 = \pi_{2+n}(S^n) = \mathbb{Z}_2$ when $n > 3$. We will see that one color exchange invariant is an invariant distinguishing two chiral subclasses of this nontrivial class.

5 Invariant as a linking number

We now construct an immersed torus, the Konstantinov torus, that is *self-linked* (Arf-Kervaire invariant one) and has a self-intersection curve with no winding components and is, hence, “ ∞ -perfect”. On this immersion, the invariant I_2 appears as a linking number.

For a q -perfect immersion, we have seen in section 3.3 that the linking numbers (with disorder parameters) are well-defined modulo q . Expand over the basis cycles to obtain,

$$LK(\mathbf{a}, \mathbf{b}) = a_x b_x lk(\mathbf{x}, \mathbf{x}) + a_y b_y lk(\mathbf{y}, \mathbf{y}) + a_x b_y lk(\mathbf{x}, \mathbf{y}) + a_y b_x lk(\mathbf{y}, \mathbf{x}) \pmod{q}. \quad (42)$$

For a self-linked immersion $q(\mathbf{x}) = lk(\mathbf{x}, \mathbf{x}) = 1$, $q(\mathbf{y}) = lk(\mathbf{y}, \mathbf{y}) = 1$ and $lk(\mathbf{x}, \mathbf{y}) = 1/2$. Multiply by 2 to obtain

$$2LK(\mathbf{a}, \mathbf{b}) = 2a_x b_x + 2a_y b_y + a_x b_y + a_y b_x \pmod{2q}, \quad (43)$$

which is precisely the Eq. (13) for I_2 , provided that $q = 2$. The immersion of Fig. 4 (b) is 1-perfect ($q = 1$), so that $2LK(\mathbf{a}, \mathbf{b})$ could be 0 or 1 and will be always 1 for the two sectors $I_2 = \pm 1$. To distinguish them, it is thus necessary to consider a different immersion with $q \geq 2$.

5.1 Construction of a Arf-Kervaire one, “ ∞ -perfect”, immersed torus

The Konstantinov torus is an immersed torus with an Arf-Kervaire invariant of one which is ∞ -perfect, originally considered by N. N. Konstantinov and described in details in Ref. [18]. For completeness, we explain how it is constructed. Consider the two sheets k and k' in Fig. 5: each is a (curvilinear) hexagon with six edges. k and k' are glued together along the three segments AB, CD, EF. After gluing, there remains three free edges from k and three free edges from k' which form a single closed curve. The two sheets overlap and are now deformed in the z direction, perpendicular to the plane of the figure. In the deformation, we push the surface towards $z \geq 0$, keeping its single edge precisely in the original plane $z = 0$. In this way, we remove most of its overlap, except for the three arcs (af) , (bc) and (de) , which are therefore part of the self-intersection curve. It is clear from the figure that the sheet k which is above k' to the left of (af) goes under k' in the central region of the figure. We immediately see that the resulting surface has a $2\pi/3$ symmetry and is chiral (no mirror plane through AB for instance), the two chiralities being obtained by selecting which of the two sheets k or k' is above the other in the central region, giving either Fig. 5 (a) or Fig. 5 (b).

In order to close the surface, we need to attach a disk to the free edge. To explain how we do this, it is convenient to attach the disk through a cylinder, which should be seen in the $z \leq 0$ part of 3d space. Fig. 6 gives several cuts of the cylinder at constant $z \leq 0$, from $z = 0$ (subfigure (9)) attached to the free edge of Fig. 5 (a), to a finite $z < 0$ (subfigure (1)) attached to a simple disk. It shows how the cylinder is folded and where the self-intersections are. To visualize the self-intersection curve, we can start from the point a at $z = 0$ and follow where the intersection point goes on the cylinder in the sequence (1)-(9) of Fig. 6. With the present choice, a goes over to b . By $2\pi/3$ symmetry, c goes to d , and e to f so that the self-intersection curve is *connected* through the remaining arcs (bc) , (de) and (fa) (there is no need to discuss the additional components on the cylinder which will not play a role in the winding properties). We can also see that there are four triple points.

The surface thus constructed is a torus. It is evident from the fact that the three sheets, k , k' and the disk can be viewed as three hexagons, on which a hexagonal lattice can be drawn:

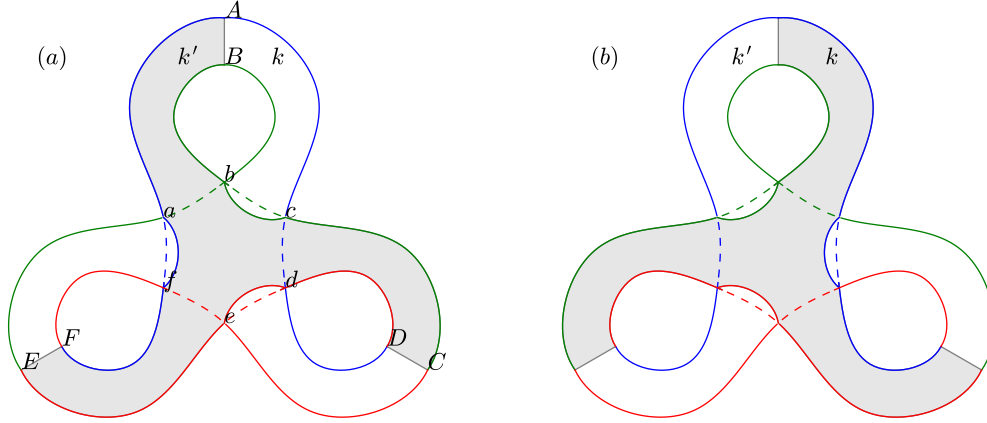


Figure 5: (a) Part of the Konstantinov torus (it is an immersed torus in 3d, here with a disk removed along the free edge): two “hexagonal” sheets k ($ADCFE B$) and k' ($ABCDEF$) glued together along AB , CD and EF , giving a sheet $k \cup k'$ with a single edge at $z = 0$ (the rest of the surface being at $z > 0$). There are three intersections along the arcs (af) , (bc) , and (ed) (solid lines), where k crosses under k' . (b) The chiral image of (a): k' crosses under k . The impossibility to connect these two immersions (a) and (b) by a 2-perfect regular homotopy provides a topological interpretation of the color exchange invariant I_2 (see section 5.2).

construct a single hexagon on each (with six dangling bonds out of it) and connect k and k' using three of these dangling bonds. The six remaining bonds of k and k' will be used to connect the six free bonds of the disk. In this case, we have $3 \times 6 = 18$ vertices, 6 edges on each piece and 6 edges for the three pairs of pieces, $3 \times 6 + 3 \times 3 = 27$ edges and 9 faces. The Euler characteristic is $\chi = V - E + F = 0$, that of a torus, indeed.

The basis cycles (the basis elements of $H_1(T^2, \mathbb{Z})$) of such an immersion are self-linked. There are three equivalent cycles (related by $2\pi/3$ symmetry) which we call x , y and z . Each has the shape of a figure eight and can be all contained in $k \cup k'$: the cycle x starts from the middle of the segment AB , for instance, and goes over to CD on k' and from CD to AB on k . Note that indeed if we cut the surface along x , it does not separate the surface into two pieces, it is therefore not the border of a surface and is a nontrivial cycle. On a torus, there are two primitive cycles and they intersect once. The second one is therefore y (which goes from CD to EF on k and back on k'), or equivalently z . Consider the tubular neighbourhood of x . The ribbon has the shape of a lemniscate (with its double point avoided in the third dimension). It is easy to see by cutting the ribbon along its middle line that the two ribbons thus obtained are *linked*, $lk(x, x') = 1$, we say that the cycle is self-linked. If, however, we look at the frame of the ribbon, we see that the binormal vector is always close to the z -axis whereas the normal and tangent vectors do not do a full turn. This element is the trivial element of $\pi_1[SO(3)]$: it can be folded as two circles one above the other and corresponds to a 4π rotation (trivial element). By symmetry, the same argument applies to y or z , so that $q(x) = q(y) = q(z) = 1$. The immersion has therefore an Arf-Kervaire invariant of one and cannot be transformed by regular homotopy onto the standard torus [17]. The self-intersection curve on the torus with the hole does not wind around, it is obvious that

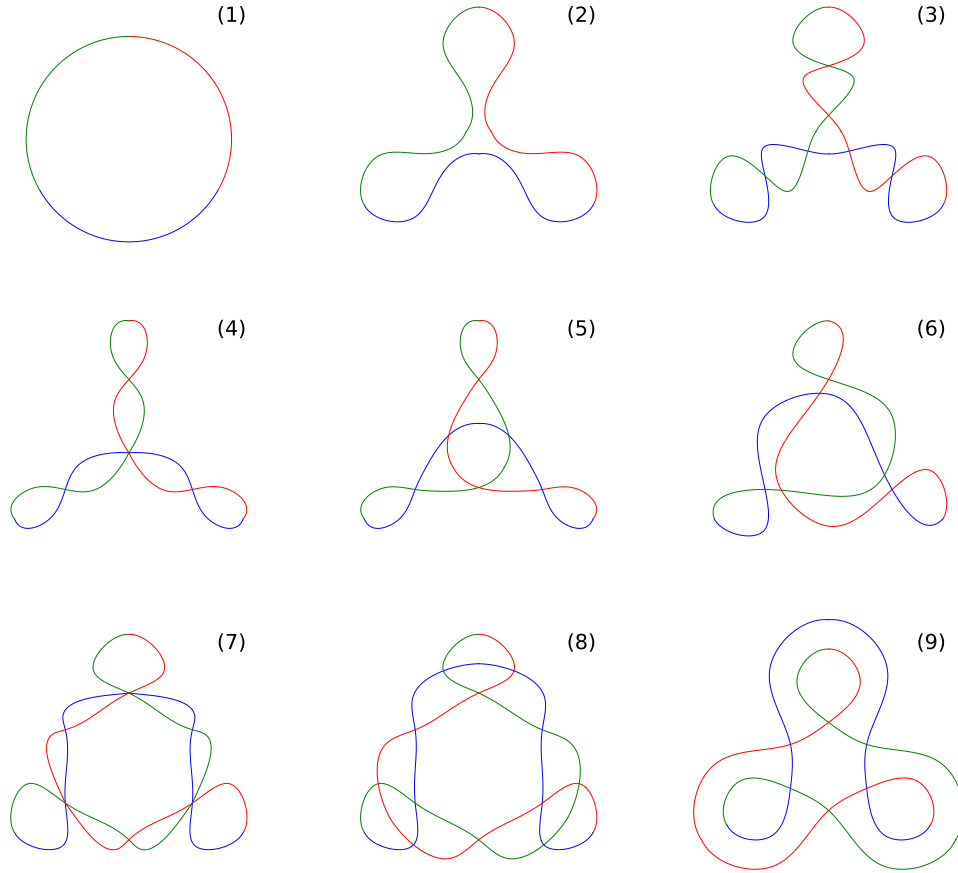


Figure 6: Several cuts of the cylinder, at different z , whose first free edge (1) will be connected to the disk and the second free edge (9) to the surface $k \cup k'$ along its $z = 0$ edge (Fig. 5). Each crossing is a double point and there are 4 triple points in (4) and (7). In between steps (5) and (7), the mirror plane perpendicular to the plane of the figure is broken: a chirality is chosen which must map the chirality of the sheet $k \cup k'$.

each arc (*e.g.* (af)) does not have an overlap with x , y or z : the self-intersection curve is homotopically trivial (all other components are closed on the disk and are similarly trivial) and the immersion is therefore ∞ -perfect. We have thus explained the construction and the properties of a Arf-Kervaire invariant one, ∞ -perfect, torus.

The Konstantinov torus is, in particular, 2-perfect, and Eq. (43) holds modulo 4. The invariant $I_2 = \pm 1$ is thus visualized as the obstruction to unlink the cycles on the Konstantinov torus.

5.2 Interpretation as a topological obstruction

We can provide a topological interpretation of the color exchange invariant I_2 , following section 3.4.

Consider the two Konstantinov torus that are image of each other by a mirror plane given

in Fig. 5 (a) and Fig. 5 (b). Note that they both have an Arf-Kervaire invariant of one, so that there exists a regular homotopy between them.

We have just explained that it is possible to construct configurations with $2LK = +1 \pmod{4}$ ($I_2 = +1$ in section 2.1) on a given Konstantinov torus and that any 2-perfect regular homotopy will not change this number. Since LK is a chiral number, it is changed in its opposite by reflections and the chiral image of the immersion will have $2LK = -1$. As we have seen in section 3.4, $2LK$ is conserved modulo 4 by a 2-perfect regular homotopy. As a consequence, there is no 2-perfect regular homotopy that will connect the two chiral Konstantinov immersions: they form new chiral classes by themselves for 2-perfect homotopies, characterized by $2LK = \pm 1$.

The nontrivial class of Π_2 thus admits subclasses, *i.e.* immersions that cannot be transformed into one another by 2-perfect regular homotopies. The color invariant $I_2 = \pm 1$ thus reflects this obstruction between two immersions, up to such deformations.

6 Conclusion

We have explained that the invariants I_2 , I'_2 and I''_2 associated with color exchange can be visualized as a linking of the Kempe loops, when properly immersed in 3d: the obstruction to the dynamics I, described by $I_2 = \pm 1$, needs to be visualized as linked winding loops on a self-linked, Arf-Kervaire one, immersed torus, while that of dynamics II described by $I'_2 = 0$ or 1, or $I''_2 = \pm 1$, appears as linking on the standard embedded torus.

An equivalence has emerged between invariants of dynamics and finer classes of homotopies or cobordism, which are the equivalence classes of “ q -perfect” regular homotopies. It reflects the possibility (or not) to connect immersions by regular homotopy or cobordism *without modifying the winding properties of the self-intersection curves*. This is this mathematical property which is equivalent (in the sense of being described by the same invariants) to the obstructions in the physical dynamics of colors.

In this sense, the obstruction in color dynamics I is thus explained by the topological obstruction to transform the immersion given in Fig. 5 (a) into its chiral image (Fig. 5 (b)), up to the continuous deformation we have defined. The color invariant thus arises as a new obstruction in Π_2 , resulting in finer chiral subclasses.

The present results call for generalizations to abstract surfaces M other than the torus T^2 . It would involve replacing the two winding numbers of a given loop by an element of the (in general, nonabelian) group $\pi_1(M)$. The dynamics would involve motion within the group and invariants may similarly exist. It could be possible to consider various immersions of the surfaces M and study the equivalence between invariants of dynamics and invariants of homotopies or cobordism. For example, the 3-color problem of the hexagonal lattice on the Klein bottle also has Kempe sectors [13]. Immersions of the Klein bottle (or, more generally, of a nonorientable surface), are characterized by the Arf-Brown invariant, defined modulo 8 (reflecting the possibilities of twists by π -turn), instead of modulo 2, as in Eq. (40). This provides further invariant properties of the immersions, representing higher-homotopy group elements. Note that immersions need not be restricted to 3d Euclidean space, and surfaces can be immersed in other 3d manifolds, giving additional possibilities. It is a question as to whether Kempe sectors may help to characterize further some regular cobordism classes.

While we have explained the correspondence between I_2 , I'_2 and linking numbers on im-

mensions (and I_1 as the parity of the number of intersections of winding loops), it is possible that the invariants I_3^\pm , $I_3^{\pm'}$ or, more generally, invariant of other similarly constrained problems, could be expressed in terms of higher invariants which are not functions of pairwise linking numbers but more general invariants or intersection forms.

References

- [1] A. B. Kempe, American Journal of Mathematics, **2**, 193 (1879).
- [2] W. T. Tutte, Proc. London Math. Soc., 50, 137–149 (1948). doi:10.1112/plms/s2-50.2.137
- [3] D. Huse and A. Rutenberg, Phys. Rev. B **45**, 7536 (1992). doi:10.1103/PhysRevB.84.020413.
- [4] A. D. Sokal, Markov Processes and Related Fields, 7, 21:38 (2000).
- [5] B. Mohar (2006), in: Bondy A., Fonlupt J., Fouquet JL., Fournier JC., Ramírez Alfonsín J.L. (eds) Graph Theory in Paris. Trends in Mathematics. Birkhäuser Basel. doi:10.1007/978-3-7643-7400-6.
- [6] M. Heinrich, *Reconfiguration and Combinatorial Games* (2019), PhD. Thesis, Université Lyon I (unpublished).
- [7] R. J. Baxter, J. Math. Phys. **11**, 784 (1970). doi:10.1063/1.1665210.
- [8] C. Moore and M. E. J. Newman, J. Stat. Phys. 99, 629-660 (2000). doi:10.1023/A:1018638624854.
- [9] O. Sikora, N. Shannon, F. Pollmann, K. Penc, and P. Fulde, Phys. Rev. B **84**, 115129 (2011). doi:10.1103/PhysRevB.84.115129.
- [10] M. Freedman, M. B. Hastings, C. Nayak, and X.-L. Qi, Phys. Rev. B **84**, 245119 (2011). doi:10.1103/PhysRevB.84.245119.
- [11] B. Mohar and J. Salas, J. Phys. A: Math. Theor. 42 (2009) 225204. doi:10.1088/1751-8113/42/22/225204.
- [12] B. Mohar and J. Salas, J. Stat. Mech. P05016 (2010). doi:10.1088/1742-5468/2010/05/P05016.
- [13] O. Cépas, Phys. Rev. B **95**, 064405 (2017). doi:10.1103/PhysRevB.95.064405.
- [14] S. Fisk, Adv. in Math. **25**, 226 (1977). doi:10.1016/0001-8708(77)90075-5.
- [15] O. Cépas and P. M. Akhmetiev, SciPost Phys. **7**, 32 (2019). doi:10.21468/SciPostPhys.7.3.032
- [16] P. M. Akhmetiev and O. Cépas, Proceedings of the Kolomna conference (2019). ISBN-978-5-98492-402-3.
- [17] U. Pinkall, Topology, **24**, 421 (1985). doi:10.1016/0040-9383(85)90013-8.

- [18] P. M. Akhmet'ev, Russ. Math. Surv. **55**, 405 (2000).
doi:10.1070/rm2000v055n03abeh000290.
- [19] A *regular* homotopy is a homotopy between immersions, *i.e.* the immersion must have tangent vectors well-defined at every point and all “times” of the deformation.
- [20] See, for example, B. A. Dubrovin, A. T. Fomenko and S. P. Novikov, Modern geometry-methods and applications, Vol. 2, page 216. Springer, Graduate Texts in Mathematics.